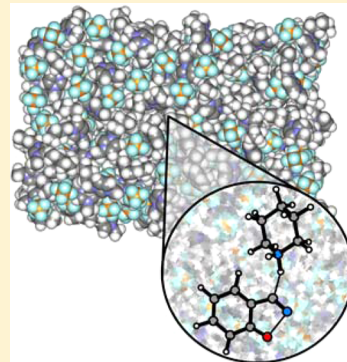


Simulating Chemical Reactions in Ionic Liquids Using QM/MM Methodology

Orlando Acevedo*

Department of Chemistry and Biochemistry, Auburn University, Auburn, Alabama 36849, United States

ABSTRACT: The use of ionic liquids as a reaction medium for chemical reactions has dramatically increased in recent years due in large part to the numerous reported advances in catalysis and organic synthesis. In some extreme cases, ionic liquids have been shown to induce mechanistic changes relative to conventional solvents. Despite the large interest in the solvents, a clear understanding of the molecular factors behind their chemical impact is largely unknown. This feature article reviews our efforts developing and applying mixed quantum and molecular mechanical (QM/MM) methodology to elucidate the microscopic details of how these solvents operate to enhance rates and alter mechanisms for industrially and academically important reactions, e.g., Diels–Alder, Kemp eliminations, nucleophilic aromatic substitutions, and β -eliminations. Explicit solvent representation provided the medium dependence of the activation barriers and atomic-level characterization of the solute–solvent interactions responsible for the experimentally observed “ionic liquid effects”. Technical advances are also discussed, including a linear-scaling pairwise electrostatic interaction alternative to Ewald sums, an efficient polynomial fitting method for modeling proton transfers, and the development of a custom ionic liquid OPLS-AA force field.



INTRODUCTION

The role of solvent has been assumed to be static in many reactions, thought to simply contribute solvation energy to the total free energy of the system. However, direct participation of a few critical solvent molecules with the reacting substrate could have significant consequences, such as, lowering the activation energy or the creation of an electric field that changes the shape of the potential energy surface.¹ Ionic liquids are a particularly interesting class of solvent that has the ability to control and accelerate an extensive number of chemical reactions.^{2–5} These characteristically room temperature molten salts are composed of an asymmetric organic cation, such as the 1-alkyl-3-methylimidazolium [RMIM] and *N*-alkylpyridinium [RPyr] cation classes (where R = M for methyl, E for ethyl, B for butyl, etc.), and a weakly coordinating anion that exhibits diffuse negative charge such as hexafluorophosphate [PF₆] or tetrafluoroborate [BF₄]. Different ion combinations (Figure 1) can dramatically alter solvent properties, including the melting point, viscosity, density, electrical conductance, solvent polarity, and gas solubility.⁶ Fine-tuning the ion components through changes in functional groups can alter the amount of localized structuring in the liquid phase, which differentiates ionic liquids from molecular solvents and solutions containing dissociated ions.^{7–10}

As a reaction medium, ionic liquids have gained significant popularity due to their ideal properties in catalysis¹¹ and organic synthesis.¹² The observed effects of ionic liquids range from weak to powerful, but an understanding of the molecular factors are largely unknown despite the numerous organic systems reported experimentally.^{2,4} Simulations have only begun to uncover the microscopic details on how these molten salts operate upon chemical reactions. A chief underlying

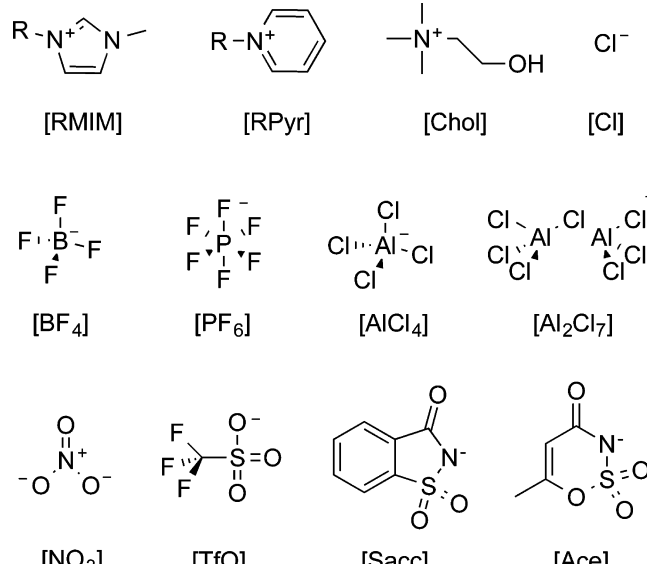


Figure 1. Ionic liquid forming ions. R = M (methyl), E (ethyl), B (butyl), H (hexyl), and O (octyl).

reason is that simulating a complex reaction medium composed entirely of ions has proven to be a considerable challenge.^{13,14} Some issues to contend with include long simulation time scales are often needed to compensate for the high viscosities of

Received: August 6, 2014

Revised: October 8, 2014

Published: October 20, 2014

ionic liquids,¹⁵ 500 or more ion pairs may be required for the proper reproduction of dynamics;¹⁶ dispersion forces are non-negligible,¹⁷ and a large number of cation and anion combinations lack experimentally validated force field parameters.¹⁸ A recent perspective by Chiappe and Pomelli advocated QM/MM as the most appropriate method for describing chemical reactivity in ionic liquids.¹⁹ The rationale was that capturing important phenomena related to global solvent structure requires a description of the bulk phase that supermolecular complexes, even coupled to continuum methods, are presently unable to achieve, e.g., reorganization of ionic liquids around the solute and the presence of polar and apolar domains.¹⁹ Our own comparisons with experimental kinetic results on medium effects has verified the accuracy of the QM/MM approach in a full range of solvents from hydrocarbons to water to ionic liquids for varied classes of organic reactions.^{20–22}

Highlighted herein are case studies of chemical reactions in ionic liquids that utilized our custom ionic liquid force field in conjunction with an on-the-fly mixed quantum and molecular mechanical (QM/MM) method coupled to Monte Carlo statistical mechanics and free-energy perturbation theory calculations (MC/FEP). Examples of organic reaction classes discussed include substitutions,²³ eliminations,^{24,25} and pericyclic.^{26,27} Detailed insight is given into the origin of the observed rate accelerations and mechanistic changes for the systems in ionic liquids compared to conventional solutions. Advances in methodology that were required to enhance the accuracy and speed of the simulations are examined. Furthermore, thoughts on necessary future improvements to our methodology are also given.

METHODOLOGICAL DETAILS AND ADVANCES

QM/MM Calculations. Combined QM/MM methods permit the modeling of bond-making and bond-breaking processes, and the treatment of systems much larger than by QM alone and/or that lack MM parameters.^{20,21,28,29} The utility of the QM/MM technique, particularly to the biomolecular simulation community, culminated in the 2013 Nobel Prize in Chemistry being awarded to Martin Karplus, Michael Levitt, and Arieh Warshel for their seminal developmental efforts and applications.³⁰ Characteristically, the solutes or key parts of the reacting system are treated with QM methods, solvent molecules are represented by MM, and the solute–solvent interactions consist of Coulombic terms using the QM and MM charges and Lennard-Jones (LJ) interactions using standard MM parameters. Monte Carlo (MC) statistical mechanics or molecular dynamics (MD) provides the sampling of the substrate and solvent molecules required to obtain configurationally averaged free-energy results. Without sufficient sampling, *ab initio* QM/MM methods have been shown to give significantly varied reaction and activation energies on similar configurations.³¹ However, extensive sampling is accompanied by the need to perform large numbers of QM calculations. Our preference has been to employ highly efficient semiempirical QM (SQM) methods, e.g., PDDG/PM3,³² AM1,³³ and RM1,³⁴ though alternative approaches exist.³⁵ Our ionic liquid QM/MM simulations have primarily utilized the PDDG/PM3 method, but the SQM MSINDO method also provided good results.³⁶

In our setup, the reacting systems are surrounded by hundreds or thousands of solvent molecules, which are included explicitly using the OPLS-AA force field.³⁷ Periodic

boundary conditions are used for the organic reactions, and the active sites of enzymes are embedded in water caps. Solute–solvent and solvent–solvent interactions are typically truncated using 10–12 Å cutoffs with smoothing over the last 0.5 Å. The energy and wave function for the QM region are obtained from single-point calculations upon each attempted MC move of a QM element. The nonbonded potential energy between the QM and MM regions is given by Coulomb and Lennard-Jones interactions where the solute is not covalently bound to the solvent region. When necessary, “capping” of the covalent bonds between the QM and MM parts of the system and treatment of bonded interactions near the interface are handled using a movable link-atom approach.^{38,39}

Our QM/MM method utilizes the Cramer–Truhlar CMx models for the calculation of charges on the QM atoms.⁴⁰ As the CMx models have been optimized for the reproduction of gas-phase dipole moments, neutral liquid-phase molecules are scaled by 1.14 to replicate experimental free energies of hydration.⁴¹ These selections provide a balanced treatment such that acceptable results are consistently obtained for medium effects on equilibria and reaction rates.

Ionic Liquid Force Field. To model ionic liquid bulk-phase effects, OPLS-AA force field parameters have been developed and validated in our lab for use in the simulation of 68 unique combinations of ionic liquids featuring [RMIM]⁺ (R = M (methyl), E (ethyl), B (butyl), H (hexyl), and O (octyl)), [RPyr]⁺, and choline cations, along with Cl[−], PF₆[−], BF₄[−], NO₃[−], AlCl₄[−], AlCl₇[−], TfO[−], saccharinate, and acesulfamate anions (Figure 1).²⁵ Although multiple ionic liquid force fields have been developed,⁴² our motivation lies in creating a reaction medium tailored toward QM/MM calculations. Charges, equilibrium geometries, and torsional Fourier coefficients were derived to reproduce gas-phase structures and conformational energetics from LMP2/cc-pVDZ(-f)//HF/6-31G(d) quantum mechanical calculations. As a brief overview, the total energy of the ionic systems are evaluated as a sum of individual energies for the harmonic bond stretching and angle bending terms, a Fourier series for torsional energetics, and Coulomb and 12-6 Lennard-Jones terms for the nonbonded interactions, see eqs 1–4. The parameters are the force constants *k*, the *r*₀ and *θ*₀ reference values, the Fourier coefficients *V*, the partial atomic charges, *q*, and the Lennard-Jones radii and well-depths, *σ* and *ε*.

$$E_{\text{bonds}} = \sum_i k_{b,i} (r_i - r_{o,i})^2 \quad (1)$$

$$E_{\text{angles}} = \sum_i k_{a,i} (\theta_i - \theta_{o,i})^2 \quad (2)$$

$$\begin{aligned} E_{\text{torsion}} = & \sum_i \left[\frac{1}{2} V_{1,i} (1 + \cos \phi_i) + \frac{1}{2} V_{2,i} (1 - \cos 2\phi_i) \right. \\ & \left. + \frac{1}{2} V_{3,i} (1 + \cos 3\phi_i) + \frac{1}{2} V_{4,i} (1 - \cos 4\phi_i) \right] \end{aligned} \quad (3)$$

$$E_{\text{nonbond}} = \sum_i \sum_{j>i} \left\{ \frac{q_i q_j e^2}{r_{ij}} + 4e_{ij} \left[\left(\frac{\sigma_{ij}}{r_{ij}} \right)^{12} - \left(\frac{\sigma_{ij}}{r_{ij}} \right)^6 \right] \right\} \quad (4)$$

The geometric combining rules regularly used for the Lennard-Jones coefficients are employed: $\sigma_{ij} = (\sigma_{ii}\sigma_{jj})^{1/2}$ and

$\epsilon_{ij} = (\epsilon_i \epsilon_j)^{1/2}$.⁴³ All individual ions (Figure 1) were optimized using the current practice for OPLS-AA parametrization.^{37,44,45} Briefly, *ab initio* derived ion geometries were used for the equilibrium bond and angle, r_0 and θ_0 , reference values in the force field. Partial charges were computed by fitting the molecular electrostatic potential (ESP) at the atomic centers. For a better description of the charge density, LMP2 dipole moments were also computed along with a coupled perturbed Hartree–Fock (CPHF) term. Charges were symmetrized for similar atoms and used for the Coulombic nonbonded force field partial charges. Torsional energies were fit to reproduce computed LMP2/cc-pVTZ(-f)//HF/6-31G(d) energy scans.

Multiple alkyl chain lengths were considered in the fitting process and the quality of the fits for the transferable force field yielded energy profiles for bond rotations comparable to that of *ab initio* calculations. In addition, the highly transferable parameters for [RMIM] and [RPyR] were compared to potentials developed specifically for individual ionic liquid cations and good accord in liquid densities and ΔH_{vap} values were found between both sets.²⁵ Relative deviations from experimental density values were ca. 1–3%, however chloroaluminate-based ionic liquids had slightly larger deviations at ca. 4–5% (Figure 2). Agreement between our

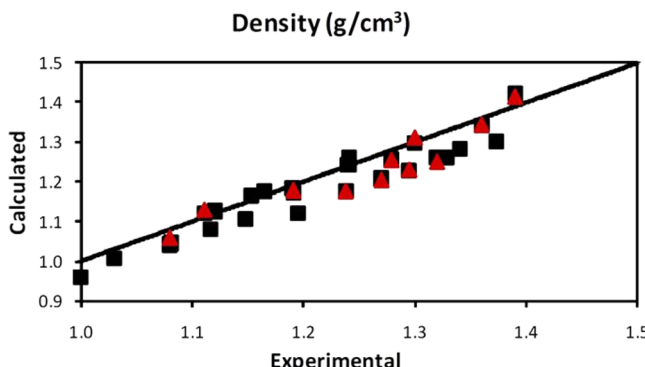


Figure 2. Computed OPLS-AA and experimental results for liquid densities for 1-alkyl-3-methylimidazolium [RMIM]-based ionic liquids (black squares) at 25 °C and 1 atm. Computed values with OPLS-AA parameters specific to [EMIM] and [BMIM] given as red triangles.

computed ΔH_{vap} and experimental estimates were reasonable and largely matched up well with those derived from other force fields.⁴² The importance of testing the cation and anion parameters in a large number of ionic liquid combinations was highlighted by an unprecedented number of 68 ionic liquid simulations.²⁵ In addition, 35 of the 68 solvents were recomputed using specific cation parameters to allow a detailed comparison of parameter transferability between different alkyl chain lengths and anion combinations.

SF3 Long-Range Electrostatics. Ionic liquid calculations require significantly more sampling than conventional solutions due to the large degree of localized structuring in the molten salts. Consequently, a large amount of computer time is required for the convergence of solvent properties, much of which is spent evaluating long-range electrostatics.⁴⁶ Ewald (or lattice) summations can provide an accurate electrostatic treatment by using a cutoff distance for the quickly decaying short-ranged real-space summation and by performing a second long-ranged reciprocal-space summation.⁴⁷ As the number of particles, N , increases, a simple Ewald implementation can increase the simulation effort as $O(N^2)$. Optimization of the

reciprocal-space summation with Fourier-based approaches can scale lower, i.e., $O(N \log(N))$.⁴⁸ Alternatively, cutoff truncation artifacts can be reduced by the use of a linear-scaling *shifted potential* scheme that provides a continuous shifting of the potential at all distances such that the value of the potential (or the value and first derivative for a *shifted force potential*) becomes zero at the cutoff distance.⁴⁹ The general shifting scheme was first proposed by Brooks, Pettitt, and Karplus⁴⁹ and implemented by Levitt et al. to treat electrostatics in biological simulations.⁵⁰ The method modifies the interactions energy by subtracting it from a truncated Taylor series of the original energy (eq 5), where $V(r_{ij})$ and $V(R_C)$ are the original potentials and equal to $1/r_{ij}$ and $1/R_C$, respectively; $dV(R_C)/dr$ is its derivative with respect to r_{ij} evaluated at the cutoff distance R_C , and r_{ij} is the distance between particles.

$$V_{n\text{-shifted}}(r_{ij}) = \begin{cases} V(r_{ij}) - V(R_C) & r_{ij} \leq R_C \\ - \sum_{m=1}^n \frac{1}{m!} (r_{ij} - R_C)^m \frac{d^m V(R_C)}{dr^m} & r_{ij} > R_C \\ 0 & \end{cases} \quad (5)$$

In our efforts to enhance the speed of computing long-range electrostatics in ionic liquid simulations, the Levitt et al. equation was expanded to the $n = 3$ case (eq 6) and called the *shifted force third derivative* (SF3) method.⁵¹ Monte Carlo simulations utilizing our OPLS-AA ionic liquid force field and employing different pairwise alternatives with multiple cutoff distances and electrostatic damping values were compared to the energetics from full Ewald sums. The SF3 method was examined on 59 unique ionic liquid combinations of [RMIM] and [RPyR] cations, along with Cl^- , PF_6^- , BF_4^- , NO_3^- , AlCl_4^- , Al_2Cl_7^- , and TfO^- anions. The SF3 method provided a significant 8- to 9-fold speed-up in the calculation time and was found to be an accurate alternative to full Ewald sums.⁵¹

$$V_{\text{SF3}} = \begin{cases} q_i q_j \left[\frac{1}{r_{ij}} - \frac{1}{R_C} + (r_{ij} - R_C) \left(\frac{1}{R_C^2} \right) \right. \\ \left. - (r_{ij} - R_C)^3 \left(\frac{1}{R_C^4} \right) \right] & r_{ij} \leq R_C \\ 0 & r_{ij} > R_C \end{cases} \quad (6)$$

Free Energy Perturbation (FEP) Theory. FEP simulations were reported over 20 years ago and early applications probed chemical and biochemical reactivity, e.g., the solvation of small molecules.^{52,53} FEP theory uses the Zwanzig expression (eq 7) to relate the free energy difference by constructing a nonphysical path connecting the desired initial (0) and final (1) state of a system.⁵⁴ For example, in our work calculating the relative free energies of binding for potential inhibitors of HIV,^{55,56} perturbations were made to convert one ligand to another using the thermodynamic cycle shown in Figure 3. The $\langle \rangle$ brackets in eq 7 indicate that the bracketed quantity is averaged over all the configurations X can adopt from $\Delta G(X \rightarrow Y)$ and are weighted by their Boltzmann probabilities. Configurations of X are generated using a molecular simulation, i.e., MD or MC statistical mechanics. A

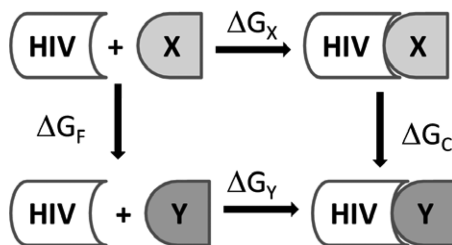


Figure 3. Thermodynamic cycle for relative free energies of binding. Host is the receptor, and X and Y are different ligands.

simple average of the exponential term is then performed over these configurations.

$$\Delta G(X \rightarrow Y) = -k_B T \ln \langle \exp[-(E_Y - E_X)/k_B T] \rangle_X \quad (7)$$

Instead of chemical mutations, free energy changes may be computed as a function of some inter- or intramolecular coordinate, e.g., a bond distance between two atoms or a dihedral angle. The free energy surface along the chosen coordinate is known as a potential of mean force (PMF). Several methods exist for carrying out PMF calculations.⁵³ In our implementation, the FEP calculation is broken into a series of intermediate steps or “windows” that is defined by a coupling parameter λ . In this way, the overall perturbation is split into multiple small steps. For each intermediate step ($\lambda_i \rightarrow \lambda_{i+1}$), the system undergoes MC statistical mechanics equilibration and averaging and the resultant free energy difference is determined. The total free energy difference for the system is the sum of all intermediate windows. Double-wide sampling is used to double the efficiency of these calculations by simultaneously calculating $\lambda_i \rightarrow \lambda_{i+1}$ and $\lambda_i \rightarrow \lambda_{i-1}$ windows.⁵⁷

PMF simulations were expanded to monitor three simultaneous reaction coordinates in our work elucidating a long-standing mechanistic controversy regarding whether the $^1\text{O}_2$ -ene reaction follows a concerted or stepwise pathway.⁵⁸ This improved the predictive capabilities of the FEP simulations by creating 3-D free-energy profiles in resemblance of 3-D and 4-D NMR experiments, where the 2-D spectrum is spread out over additional dimensions. The usefulness of the multidimensional computational technique has proven powerful by underscoring the inherent dangers of defining valley-ridge inflection points on potential energy surfaces using a limited number of reaction coordinates.⁵⁸

Proton-Transfer Polynomial Method. We reported a significant technical advance for the treatment of proton-

transfer reactions in both organic and enzymatic systems, where it was found that free energy changes for individual windows can be fit almost perfectly by a polynomial (Figure 4).^{38,59,60} For a typical proton transfer, e.g., $\text{O}-\text{H} \cdots \text{O}' \rightarrow \text{O} \cdots \text{H}-\text{O}'$, it was found that the $\text{O} \cdots \text{O}'$ distance remains relatively constant and that $r(\text{O}-\text{H}) - r(\text{H}-\text{O}')$ can be used to compute a 1-D PMF. This requires minimally 30 double-wide FEP windows using 0.02 \AA Δr increments, whereas ca. 900 windows would be needed for a 2-D PMF using two distances as reaction coordinates. In our method, 7 windows were fit instead with a polynomial and analytically integrated to yield the overall proton-transfer PMF (Figure 4).⁵⁹

For a specific example, Figure 5 features two different proton transfers between 5-nitrobenzisoxazole and acetate acting as a base in a periodic box of 740 TIP4P⁶¹ water molecules, and 5-nitrobenzisoxazole in antibody 4B2 using the previously described methodology.⁶⁰ In viewing Figure 5, it is immediately clear that a greater level of accuracy is obtained relative to the full 50 window “exact” PMF simulation when the free-energy profile is computed using a fifth-order polynomial compared to a cubic polynomial. Higher order polynomials were also tested but were found to give nearly identical energies and polynomial fits (ca. $R^2 = 0.999$ to the seven windows) as the fifth order. The computed ΔG^\ddagger of 25.6 kcal/mol for the Kemp elimination of 5-nitrobenzisoxazole by acetate in water is in good agreement with the experimentally measured value of 23.8 kcal/mol.⁶² Typical deviations in ΔG^\ddagger between the approximate and the detailed calculations range from 0.5 to 1 kcal/mol. However, the approximate 7-fold improvement in computational efficiency (and close to 50-fold increase for double proton transfers) compared to that for traditional PMF methods may warrant the accompanying error. The fifth-order polynomial method has been applied to a wide variety of reaction types, example reactions include a Kemp elimination,⁶⁰ a β -elimination,²⁴ and an antibody-catalyzed aldol reaction.³⁹ Some of the reactions are discussed in greater detail below.

■ ELUCIDATING SOLVENT EFFECTS ON CHEMICAL REACTIONS

Kemp Elimination. The free-energy surface for the Kemp elimination of benzisoxazole via piperidine (Scheme 1) was computed in 1-butyl-3-methylimidazolium hexafluorophosphate, $[\text{BMIM}]^+[\text{PF}_6]^-$, as the first test for our ionic liquid force field to appropriately model the reaction medium in a QM/MM environment.²⁵ A 2-D PMF free energy surface was

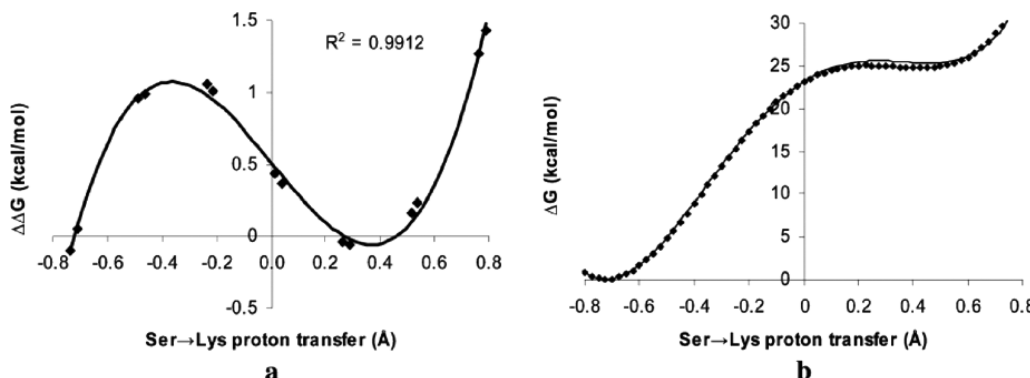


Figure 4. For proton transfers, the changes in ΔG for seven individual windows (a) fitted by a cubic polynomial, which is integrated analytically to give the full PMF (b, solid line). The “exact” PMF using 33 windows is shown for comparison (b, dotted line).

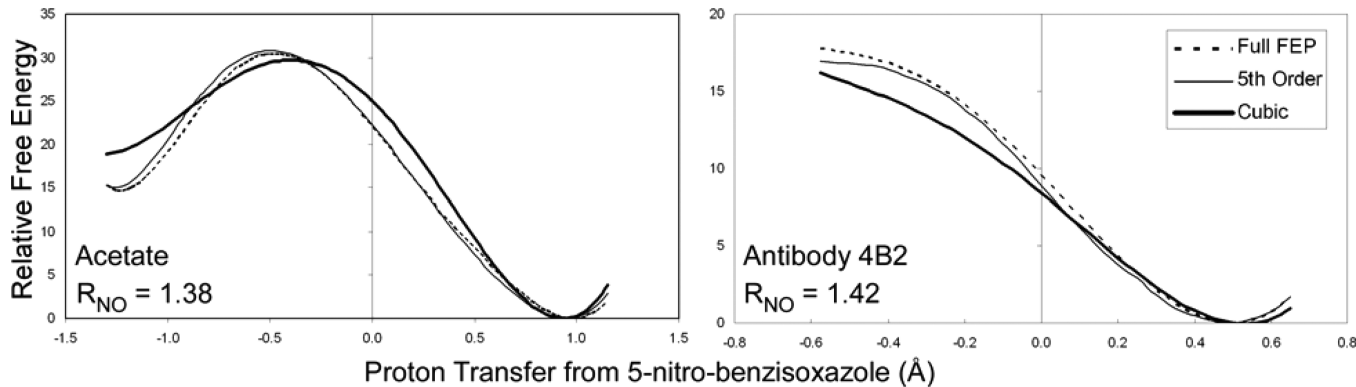
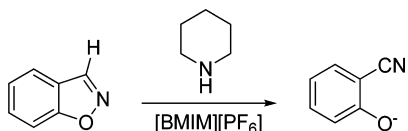


Figure 5. Proton transfers from 5-nitrobenzisoxazole to acetate (left) and antibody 4B2 (right) in water. The changes in ΔG (kcal/mol) are computed using the cubic and fifth-order polynomial methods, and the “exact” PMF using 50 windows. All distances in \AA .

Scheme 1. Kemp Elimination Reaction of Benzisoxazole with Piperidine



created by combining the proton abstraction by piperidine, $R_{\text{NH}} - R_{\text{CH}}$, with the ring opening of the benzisoxazole ring, R_{NO} , along two reaction coordinates (Figure 6). The reaction

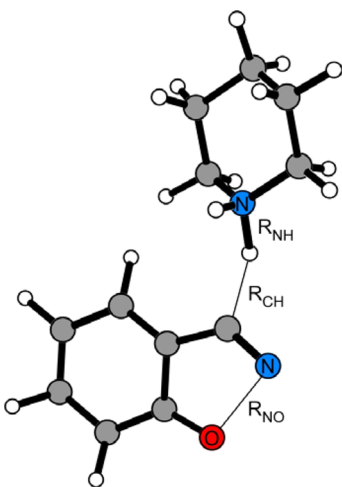


Figure 6. Illustrated structure corresponds to the QM/MM computed transition state for the Kemp elimination of benzisoxazole using piperidine in the ionic liquid [BMIM][PF₆].

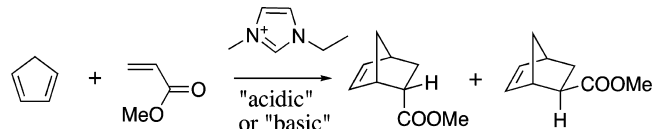
followed a concerted mechanism where the R_{NO} transition state distance was 2.06 \AA whereas the R_{NH} and R_{CH} distances were 1.10 and 1.75 \AA , respectively. Computed changes in free energy yielded a ΔG^\ddagger value of 25.2 ± 1 kcal/mol compared to an experimental ΔG^\ddagger of 22.6 ± 0.5 kcal/mol for the reaction under similar conditions.⁶³ The calculations reproduced the activation values well, particularly in light of the computed and experimental uncertainties and the additional ~ 1 kcal/mol overestimation from the fifth-order polynomial methodology.

The solvent effects on the piperidine-promoted Kemp elimination of benzisoxazole are subtle as D’Anna et al. reported experimental ΔG^\ddagger values of 22.8, 22.6, and 22.0 kcal/mol in water, [BMIM][PF₆], and DMF, respectively.⁶³ This is

in stark contrast to the large rate acceleration observed for the acetate-catalyzed elimination of 5-nitrobenzisoxazole in acetonitrile relative to water (exptl. ΔG^\ddagger of 13.1 versus 23.8 kcal/mol).⁶² Our QM/MM method predicted a ΔG^\ddagger of 25.6 kcal/mol for the aqueous-phase reaction between acetate and 5-nitrobenzisoxazole.⁶⁰ Protic solvents stabilize the base through hydrogen bonding, resulting in slower elimination rates than for aprotic solvents.⁶⁴ Accordingly, rate differences between acetate and piperidine can be attributed directly to differences in pK_a strengths. For example, the pK_a values of 4.8 and 22.3 for acetate in water and acetonitrile,⁶⁵ respectively, correlate well with the solvent-dependent Kemp elimination rates. Although ionic liquids have been shown to manipulate the effective nucleophilicity of amines,⁶⁶ the smaller pK_a variances for amines in solution, e.g., butylamine with a pK_a of 10.8 in H₂O versus 18.3 in CH₃CN,⁶⁷ limits the effectiveness of solvent-dependent rate enhancements.

Diels–Alder Reaction. The impact of ionic liquid 1-ethyl-3-methylimidazolium chloride melts ([EMIM][Cl]–AlCl₃) upon cyclopentadiene and methyl acrylate Diels–Alder reaction rates has been investigated using QM/MM calculations (Scheme 2).²⁶ An attractive property of using AlCl₃ is

Scheme 2. Diels–Alder Reaction between Cyclopentadiene and Methyl Acrylate Giving *Endo* and *Exo* Bicyclic Products in [EMIM] Chloroaluminate-Based Ionic Liquid Solvents



that the Lewis acidity of the melt can be varied with the composition of the liquid.^{4,68} For example, when AlCl₃ comprises <50% mol of the [EMIM][Cl]–AlCl₃ melt, [AlCl₄⁻] is the only chloroaluminate anion present and is called a “basic melt.” A ratio >1:1 AlCl₃ to [EMIM][Cl] is referred to as an “acidic melt” and [AlCl₄⁻] and [Al₂Cl₇⁻] are the principal anionic constituents in this case. When an acidic melt (51% AlCl₃) was used as the solvent for the Diels–Alder reaction shown in Scheme 2, the rate of reaction was 10, 175, and 560 times faster than in water, ethylammonium nitrate, and 1-chlorobutane, respectively.⁶⁹ However, the basic melt (48% AlCl₃) gave a rate 2.4 times slower than that of water.

Our QM/MM computed $\Delta\Delta G^\ddagger$ (kcal/mol) values of 0.0, +0.6, and -2.9 in water, [EMIM][AlCl₄⁻], and [EMIM]-

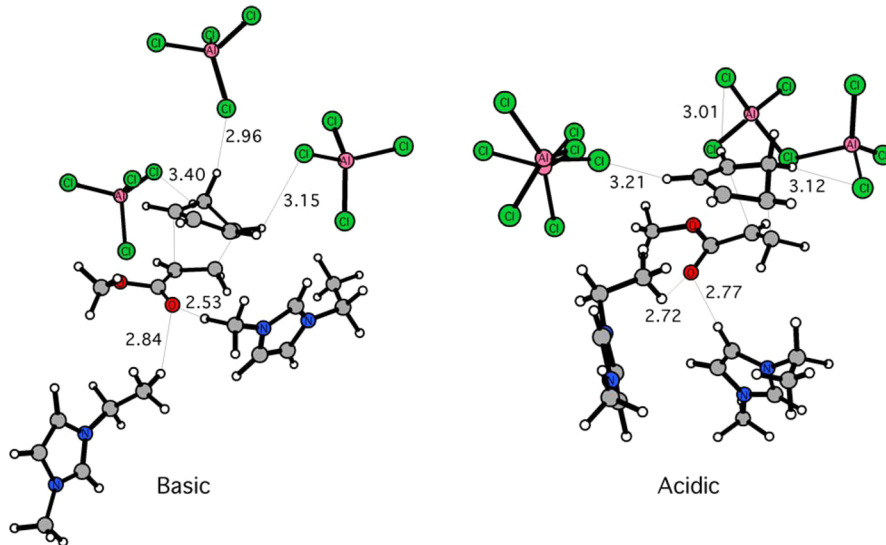
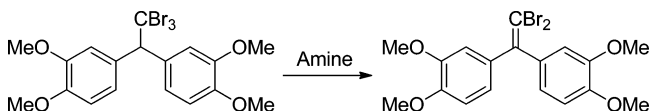


Figure 7. Typical snapshots of transition states for the Diels–Alder reaction in the “basic” $[\text{EMIM}][\text{AlCl}_4]$ and “acidic” $[\text{EMIM}][\text{Al}_2\text{Cl}_7]$ melts (only nearest ions are illustrated). Average distances (\AA) are given from 10 million overall Monte Carlo configurations of QM/MM simulations.

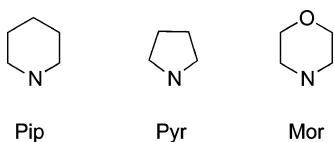
$[\text{Al}_2\text{Cl}_7]$, respectively, mirrored well the experimental values of 0.0, +0.52, and -1.36^{26} . The qualitative picture that emerges is that the reaction rate is greater in the acidic rather than the basic melt because ion-pairing is less dominant in the acidic melt (Figure 7). The relative stabilization of the transition state through hydrogen bonding with the $[\text{EMIM}]$ cation in the acidic melt is also greater than that afforded by the weaker Lewis-acid effect provided by hydrogen bonding with water molecules in aqueous solution.⁷⁰ A DFT-based supermolecular approach that complexed the same Diels–Alder reaction to a single $[\text{EMIM}]$ cation with one or two $[\text{AlCl}_4]$ and/or $[\text{Al}_2\text{Cl}_7]$ anions confirmed the same trends and conclusions as the QM/MM calculations.^{27,71} The ability of the ionic liquid to act as a hydrogen bond donor (cation effect), moderated by its hydrogen bond accepting ability (anion effect) may also explain observed *endo/exo* ratios.⁷²

β -Elimination. A change in mechanism for both a nucleophilic displacement reaction⁷³ and a base-induced β -elimination⁷⁴ has been reported to occur as a direct consequence of ionic liquid solvation. In the case of the fundamentally important β -elimination between 1,1,1-tribromo-2,2-bis(3,4-dimethoxyphenyl)ethane and the cyclic amines piperidine and pyrrolidine (Schemes 3 and 4), the reaction

Scheme 3. β -Elimination Reaction of 1,1,1-Tribromo-2,2-bis(3,4-dimethoxyphenyl)ethane

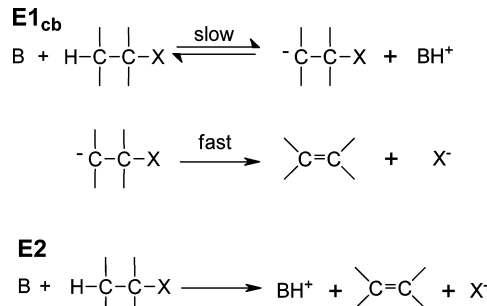


Scheme 4. Cyclic Amine Nucleophiles: Piperidine (Pip), Pyrrolidine (Pyr), and Morpholine (Mor)



transforms from an irreversible E1cb mechanism in methanol⁷⁵ to an E2 reaction pathway in the $[\text{BMIM}][\text{BF}_4]$ and $[\text{BMIM}][\text{PF}_6]$ ionic liquids.⁷⁴ In the concerted E2 mechanism, the amine abstracts the β -hydrogen with concurrent cleavage of the α -C–Br bond; in contrast, the E1cb process requires two separate steps that finds the abstraction of the β -hydrogen to be rate limiting and often reversible (Scheme 5).¹ However,

Scheme 5. E1cb and E2 Elimination Mechanisms



distinguishing between the irreversible E1cb and E2 mechanisms can be particularly difficult for dehydrohalogenation reactions despite their obvious differences.⁷⁶ In our work, QM/MM simulations for the β -elimination in methanol, $[\text{BMIM}][\text{BF}_4]$, and $[\text{BMIM}][\text{PF}_6]$ were carried out to investigate the mechanism change proposed by D’Anna and co-workers and its origins.²⁴ Free energy surfaces were calculated (Figure 8) by utilizing our fifth-order polynomial quadrature method for the proton transfer occurring between the nitrogen on the amine (i.e., piperidine or pyrrolidine) and the reacting hydrogen on the solute, $R_{\text{NH}} - R_{\text{HC}}$; an additional perturbation, R_{CB} , entailed breaking of the carbon-bromide bond.

The computed free energy surfaces confirmed a change in mechanism dependent upon solvent. However, a notable exception to D’Anna’s proposal is that the reaction followed an E1cb-like mechanism in methanol, that is, E2 with a significant amount of E1cb character, as no carbanion intermediate was located throughout the simulation. The findings concur with previous experimental studies of border-

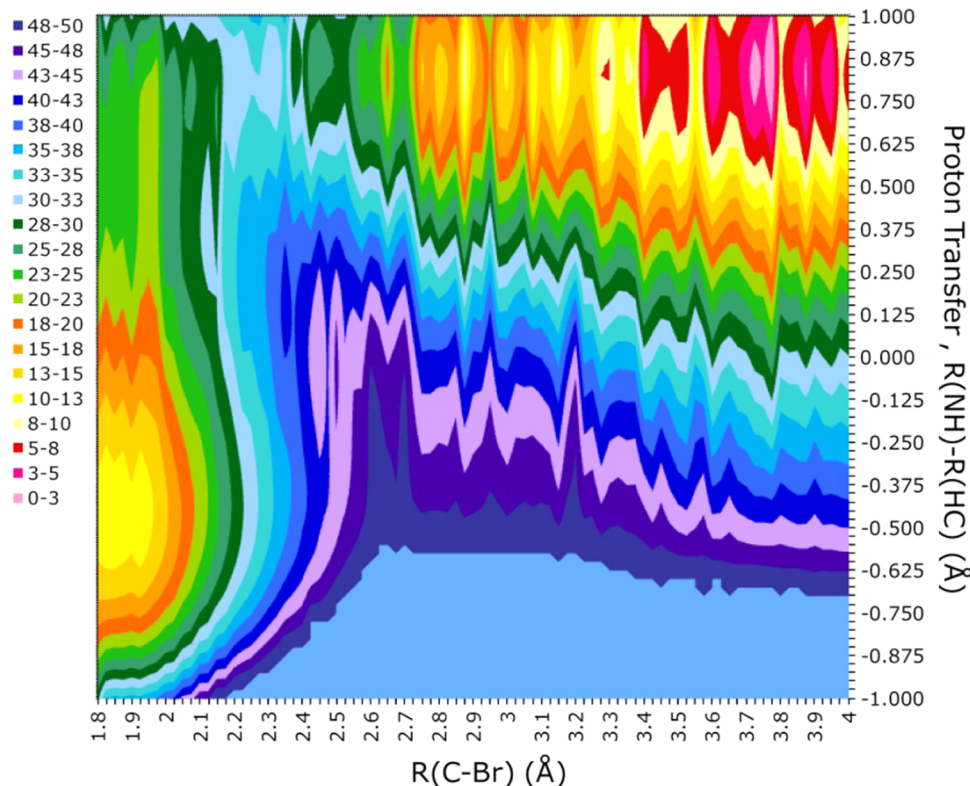


Figure 8. Free energy map (kcal/mol) computed for the β -elimination of 1,1,1-tribromo-2,2-bis(3,4-dimethoxyphenyl)ethane with piperidine in methanol. QM/MM energy values are truncated after 50 kcal/mol for clarity.

line cases between E2 and E1cb mechanisms^{77,78} (Figure 9) and were further verified by using a DFT method coupled to

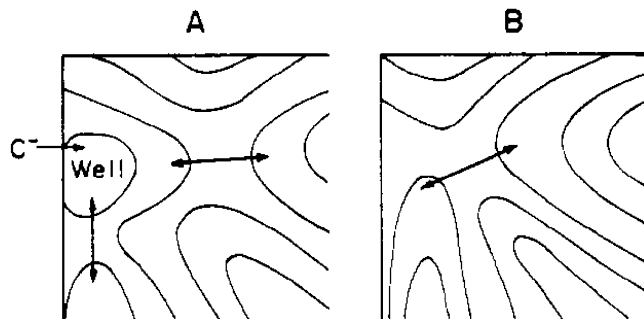


Figure 9. Hypothetical reaction coordinate contour diagram devised by Gandler and Jencks⁷⁷ to illustrate the conversion from an E1cb mechanism with a carbanion intermediate (A) to a concerted E2 mechanism when the carbanion no longer exists (B).

continuum solvent model, i.e., M06-2X/CPCM.²⁴ The structural configuration of the ions (Figure 10) plays a major role, where beneficial electrostatic interactions and $\pi^+ - \pi$ interactions between the [BMIM]⁺ cation and β -phenyl substituents were principal contributors to the mechanism change. The number of solute–solvent interactions increased by 1–3 ions when proceeding from the reactants to transition state. Additionally, the average strength of the most favorable interactions shifted to a lower energy at the transition state, in particular for pyrrolidine, which could explain its observed rate enhancement versus piperidine.⁷⁴ The BMIM cations formed a cage-like arrangement around the solute that maximized the $\pi^+ - \pi$ electronic effects exerted on the reaction route by

enforcing a coplanar orientation of the β -phenyl rings at the transition state. Monitoring the average torsions defined in Figure 11 over the final 10 million MC configurations determined the phenyl rings spend minimally 70% of the simulation in the coplanar configuration and 30% in a t-shaped configuration. In contrast, a t-shaped conformation was adopted for virtually 100% of the simulation in methanol.

S_NAr. Ionic liquids generally favor nucleophilic substitutions over base-induced eliminations. For example, nucleophilic aromatic substitution (S_NAr) reactions, which can be particularly sensitive to medium effects,^{79,80} have been reported to derive sizable rate enhancements from the ionic liquids [BMIM][BF₄] and [BMIM][PF₆]^{81,82} relative to conventional solvents. The S_NAr reaction between cyclic secondary amines (i.e., piperidine, pyrrolidine, and morpholine given in Scheme 4) and the 2-L-5-nitrothiophene (*para*-like) and 2-L-3-nitrothiophene (*ortho*-like) isomers, where L = bromo, methoxy, phenoxy, and 4-nitrophenoxy, has been computationally investigated to determine the origin of the reactivity enhancement observed in the molten salts. The S_NAr reaction follows an addition–elimination mechanism where nucleophilic attack on the *ipso* carbon forms an intermediate Meisenheimer complex followed by cleavage of the C–L bond (Scheme 6). The addition portion of the mechanism has been experimentally determined as the rate-limiting step⁸¹ and was the focus of our QM/MM calculations. The ΔG^\ddagger for the S_NAr reaction was computed by perturbing the R_{CN} distance between the reacting *ipso* carbon of the solute and the amine nitrogen in increments of 0.02 Å using our QM/MM MC/FEP methodology (Figure 12). Reasonable activation barriers differences were computed when compared to experimental thermodynamic measurements (Table 1). The error bars in the ionic

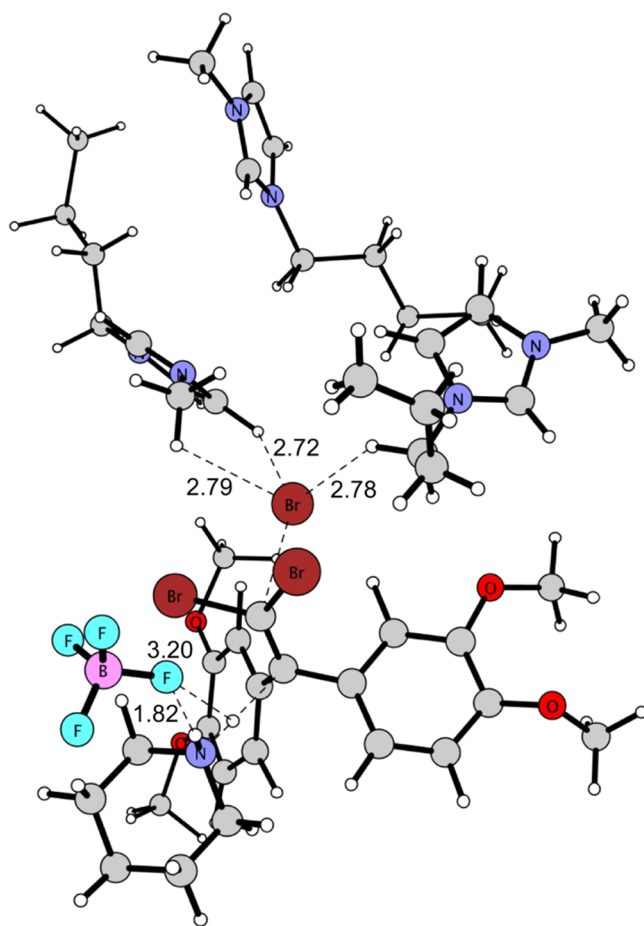


Figure 10. Typical snapshot of a transition state for the β -elimination with piperidine in $[\text{BMIM}][\text{BF}_4]$. The distances (\AA) are average values over the final 10 million configurations of QM/MM simulations. Only nearby ions are retained for clarity.

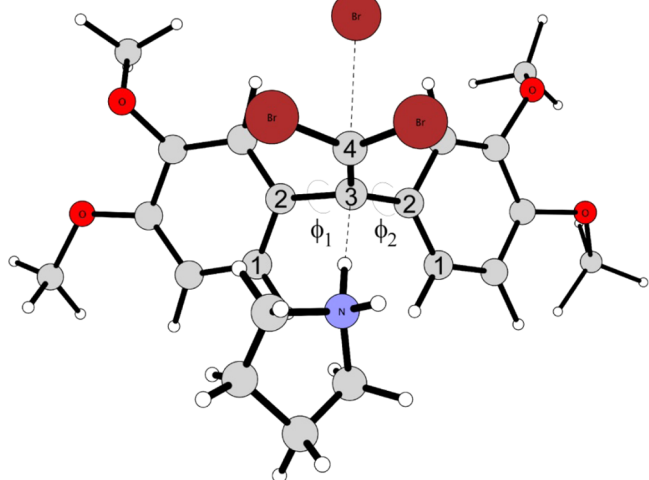
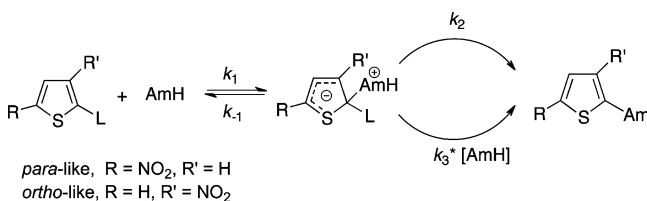


Figure 11. Transition state for the β -elimination between 1,1,1-tribromo-2,2-bis(3,4-dimethoxyphenyl)ethane and pyrrolidine in $[\text{BMIM}][\text{PF}_6]$ from the QM/MM calculations.

liquids simulations are estimated at ± 1.5 kcal/mol and experimental error bars are reported to be as large as ± 1 kcal/mol.⁸¹

Beneficial ionic liquid effects on $S_{\text{N}}\text{Ar}$ reactivity can be attributed to multiple factors including (1) an enhanced

Scheme 6. Addition–Elimination Mechanism between 2-L-5-nitrothiophene (Para-like) or 2-L-3-nitrothiophene (Ortho-like) Isomer and a Cyclic Amine (AmH) Involving the Formation of an Intermediate Meisenheimer Complex^a



^aThe leaving groups are L = Br, OCH_3 , OC_6H_5 , and $\text{OC}_6\text{H}_4\text{-}4\text{-NO}_2$.

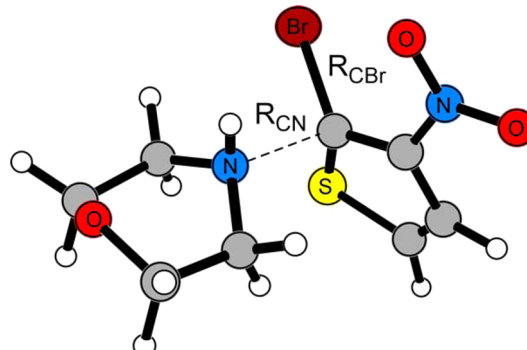


Figure 12. Snapshot of a QM/MM computed $S_{\text{N}}\text{Ar}$ transition state between morpholine and 2-bromo-3-nitrothiophene in $[\text{BMIM}][\text{BF}_4]$.

Table 1. Free Energy of Activation, ΔG^\ddagger (kcal/mol), Calculated at 25 °C for the $S_{\text{N}}\text{Ar}$ Reactions between the 2-L-5-nitrothiophene (Para-like) Isomers and Piperidine in Methanol and Ionic Liquids (Experimental Energies in Parentheses)^a

leaving group (L)	$\Delta G^\ddagger{}^b$ CH_3OH	ΔG^\ddagger CH_3OH^c	$\Delta G^\ddagger{}^b$ $[\text{BMIM}]$ $[\text{BF}_4]$	$\Delta G^\ddagger{}^b$ $[\text{BMIM}]$ $[\text{PF}_6]$
Br	25.7 (26.0)	30.8	25.8 (23.0)	25.1
OCH_3	26.5 (23.6)	30.7	27.6 (21.8)	26.2
OC_6H_5	25.1	30.5	23.8 (22.1)	26.0
$\text{OC}_6\text{H}_4\text{-}4\text{-NO}_2$	24.5 (24.1)	29.4	24.1 (21.5)	29.1

^aReference 81. ^bPDDG/PM3/OPLS-AA and MC/FEP. ^cDFT = B3LYP/6-311++G(2d,p)/PCM optimization.

nucleophilicity of the cyclic amines with an order of Pyr \geq Pip $>$ Mor, (2) favorable $\pi^+ - \pi$ interactions between the BMIM cations and the aromatic rings present on the substrate that can potentially enforce a coplanarity similar to what was found for the β -elimination, and (3) significant electrostatic enhancements between the solvent and the developing charge separation forming at the transition state (and at the intermediate Meisenheimer complex) compared to the case for the reactants. A highly ordered ionic liquid structure was again found to deliver site-specific hydrogen bonding stabilization that, despite an entropy penalty, provided a 5 kcal/mol reduction in ΔH^\ddagger compared to that for methanol.⁸¹ The encapsulation of the addition step transition state and the Meisenheimer intermediate finds 8–9 ions that are within 3 Å. Figure 13 illustrates the $[\text{BMIM}][\text{BF}_4]$ ions forming a cage-like structure to favorably interact with the substrates.

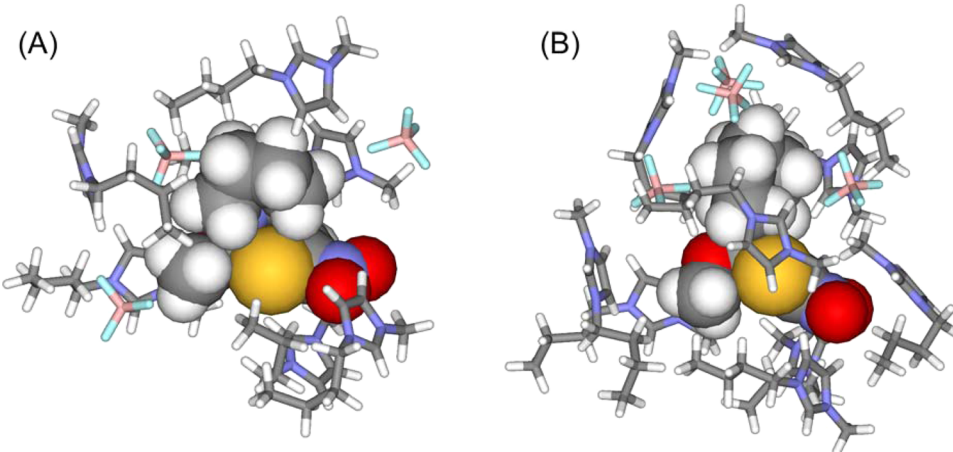


Figure 13. Illustration of first-solvation shell $[\text{BMIM}]^+ \text{[BF}_4^-]$ (shown as sticks) encapsulation of the (A) addition transition state and (B) the Meisenheimer intermediate, for the $\text{S}_{\text{N}}\text{Ar}$ reaction between piperidine and 2-methoxy-5-nitrothiophene (given as CPK space-filling model).

Again and again, detailed analyses of solute-solvent interaction energies from varied organic classes, i.e., eliminations, substitutions, and ring-forming reactions, find that the high degree of localized structuring in the liquid phase significantly contribute to the special “ionic liquid effects” observed.^{83,84} However, exploiting this understanding to predict new ionic liquids that give optimal rate and stereoselectivity enhancements for new classes of organic reactions will require continual improvement in simulation methodology.

FUTURE METHODOLOGICAL ADVANCES NEEDED

Ab Initio QM/MM. An obvious area for improvement in our QM/MM methodology is the inclusion of *ab initio* methods instead of semiempirical QM. Of course, many groups have already incorporated both wave function- and DFT-based QM methods into mixed schemes.^{85–87} Some examples, similar to our on-the-fly QM/MM method, include the recent coupling of Jorgensen’s BOSS software⁸⁸ to the versatile Gaussian QM package,⁸⁹ and the use of the PUPIL interface to link AMBER and Gaussian.⁹⁰ Nevertheless, our typical investigations of organic and enzymatic systems entail ca. 500 million single-point QM calculations over the course of each reaction pathway.^{20–22} Therefore, the incorporation of higher-level QM methods has generally required a truncation of the chemically reacting region or a reduction in the overall sampling of the system, both of which can lead to spurious findings.³¹ To overcome these limitations, both algorithmic improvements and computer hardware advances will likely be necessary, e.g., specialized QM/MM codes that take advantage of highly parallel, cost-effective coprocessors such as graphics processing units (GPUs).⁹¹

Polarization Effects. The strong ion–molecule interactions that develop at the charge-separated transition states implies that a polarizable force field may be required for proper treatment of solvent effects, particularly in low-dielectric media. For example, relative rates in cyclohexane, and to a certain extent CCl_4 , were determined to be greatly underestimated for the Menshutkin reaction between triethylamine and ethyl iodide (Scheme 7) when the nonpolarizable OPLS force field was used.⁹² Employing inducible dipoles to account for solvent polarizability yielded a dramatic effect on the ΔG^\ddagger with differences of up to 10 kcal/mol in the Menshutkin reaction compared to the case with a fixed-charge force field.⁹² Our

Scheme 7. Menshutkin Reaction between Triethylamine and Ethyl Iodide



methodology utilized a first-order polarization model, where the electric field that determines the inducible dipoles is computed from the permanent charges using eq 8 and the polarization energy is given by eq 9. As the induced dipoles do not contribute to the electric field, an iterative solution for the dipoles is not required.

$$\vec{\mu}_i = \alpha_i \vec{E}^0 \quad (8)$$

$$E_{\text{pol}} = -(1/2) \sum_i \vec{\mu}_i \cdot \vec{E}_i^0 \quad (9)$$

Polarizable ionic liquid models, e.g., utilizing self-consistent inducible dipoles^{93,94} or Drude oscillators,⁹⁵ have been shown to give major improvements to the description of dynamics.^{96,97} Still, the positive gains are counterbalanced by a significant increase in required computer resources. An alternative, cost-effective approach to account for polarization effects is the scaling of atomic charges to mimic the average charge screening caused by the polarization as well as the charge-transfer effects. Morrow and Maginn first reported a partial charge assignment of the gas-phase $[\text{BMIM}]^+ \text{[PF}_6^-]$ ion pair to be a noninteger molecular charge of ± 0.904 e;⁹⁸ subsequent work determined a molecular charge of ± 0.8 e to be ideal for reproducing experimental ionic liquid-phase properties including enthalpy of vaporization, surface tension, ion diffusion coefficients, and density.^{99,100} However, Schröder noted major discrepancies at the local level between the scaled charges and polarizable models, e.g., radial distribution functions below distances of 8 Å.¹⁰¹ This brings into question the usefulness of down-scaling solvent charges in QM/MM chemical reaction studies; investigation is currently underway in our lab.

Mixed Solvents. Ionic liquids are hygroscopic and can absorb a significant amount of water from the atmosphere.¹⁰² Experimental studies have shown that physical properties, e.g., viscosity and density, can be significantly impacted by the inclusion of water¹⁰³ and organic reactions may yield different rates, selectivity, or products depending on the presence of

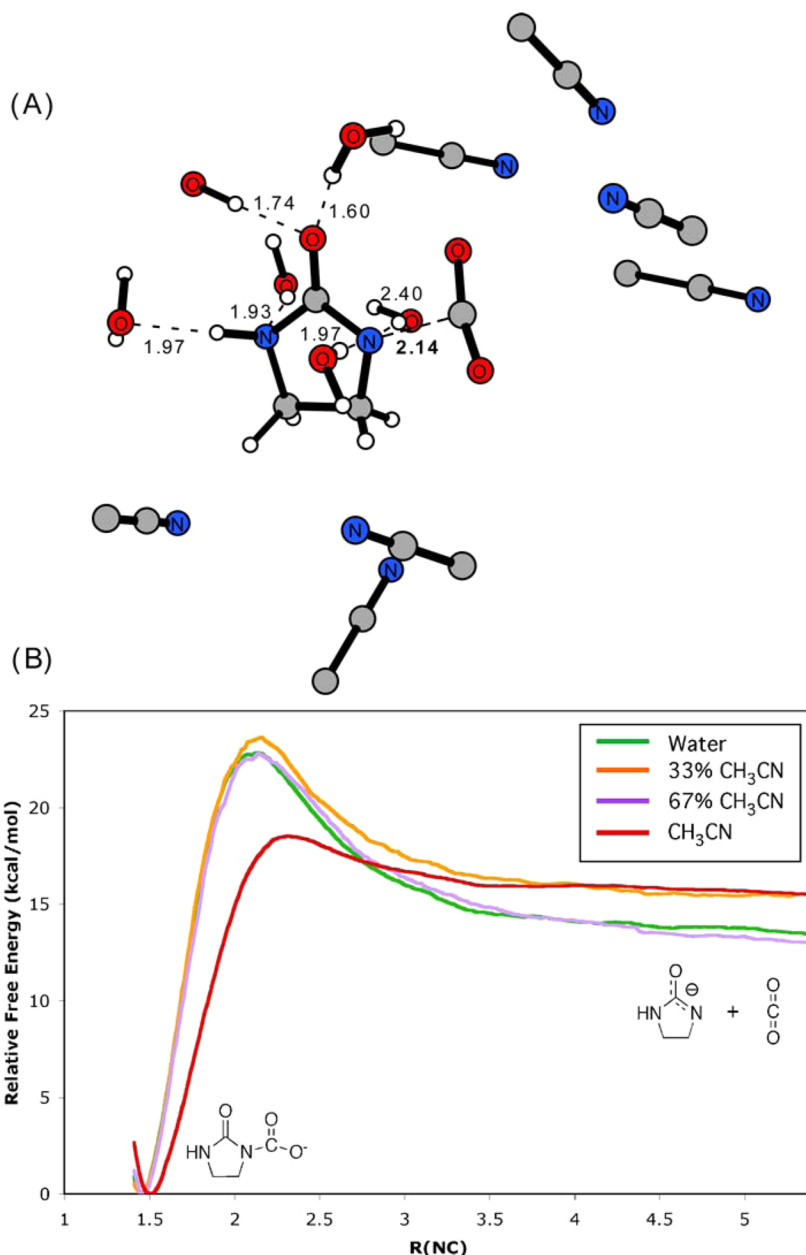


Figure 14. (A) Decarboxylation of imidazolidin-2-one-1-carboxylate anion in a 67% aqueous acetonitrile. Nearby water and acetonitrile molecules are retained; distances in Å. (B) Computed free energy profiles in pure water, 33% and 67% acetonitrile mixtures, and pure acetonitrile for the decarboxylation of imidazolidin-2-one-1-carboxylate anion.

water in the molten salts, e.g., palladium-based oxidation of toluene in [BMIM][BF₄] produced either benzaldehyde or benzoic acid depending on aqueous concentration.¹⁰⁴ Incorporating water into ionic liquid simulations should provide a more realistic QM/MM environment for computing reactions, as theoretical work on ionic liquid-water mixtures has yielded valuable insight into the solvents.^{105–108} We reported the first QM/MM MC/FEP simulation in mixed solvents for the decarboxylation of imidazolidin-2-one-1-carboxylate anion in acetonitrile:water and methanol:water mixtures, where the expected experimental pattern was reproduced with decreasing barrier heights as the percentage of water decreased (Figure 14).¹⁰⁹ Currently under investigation in our lab is a joint experimental and theoretical study on a Michael addition found to yield different products depending on the solvent chosen; we hypothesize a rate-limiting water-assisted proton transfer is in

operation in the ionic liquid solutions, emphasizing the importance of a properly modeled systems.

CONCLUSIONS

The present paper highlighted several QM/MM-based studies of chemical reactions in ionic liquids that provided deeper insight into using room temperature molten salts as the reaction medium. Novel methodological advances that improved the accuracy and speed of the simulations were discussed. Explicit solvent representation provided the medium dependence of the activation barriers and atomic-level structural detail for characterization of the nature of the “ionic liquid effect” in multiple important organic reactions. Nevertheless, significant challenges remain when it comes to properly addressing the intricacies of the molten salts. Continual improvements to the methodology beyond those

described here, for example, adaptive QM/MM methods,¹¹⁰ *ab initio* MD,¹¹¹ and enhanced trajectory analyzers,¹¹² will be needed to expand into more complex systems, such as chemical catalysis via N-heterocyclic carbene formation in imidazolium-based ionic liquids.¹¹³

AUTHOR INFORMATION

Corresponding Author

*E-mail: orlando.acevedo@auburn.edu.

Notes

The authors declare no competing financial interest.

Biography



Orlando Acevedo received a B.S. (1998) in Chemistry from Florida International University and a Ph.D. (2003) in Chemistry from Duquesne University. He was a postdoctoral associate at Yale University (2003–2006) in the laboratory of Prof. William L. Jorgensen. He joined the Department of Chemistry and Biochemistry at Auburn University in 2006 and is currently the S. D. and Karen H. Worley Associate Professor.

ACKNOWLEDGMENTS

Gratitude is expressed to the National Science Foundation (CHE-1149604) and the Alabama Supercomputer Center for support of this research. The author is indebted to the co-workers at Auburn and external collaborators.

REFERENCES

- (1) Reichardt, C.; Welton, T. *Solvents and Solvent Effects in Organic Chemistry*, 4th ed.; Wiley-VCH: Weinheim, Germany, 2011.
- (2) Hallett, J. P.; Welton, T. Room-Temperature Ionic Liquids: Solvents for Synthesis and Catalysis. 2. *Chem. Rev.* **2011**, *111*, 3508–3576.
- (3) Hubbard, C. D.; Illner, P.; van Eldik, R. Understanding Chemical Reaction Mechanisms in Ionic Liquids: Successes and Challenges. *Chem. Soc. Rev.* **2011**, *40*, 272–290.
- (4) Welton, T. Room-Temperature Ionic Liquids. Solvents for Synthesis and Catalysis. *Chem. Rev.* **1999**, *99*, 2071–2083.
- (5) Yau, H. M.; Keaveney, S. T.; Butler, B. J.; Tanner, E. E. L.; Guerry, M. S.; George, S. R. D.; Dunn, M. H.; Croft, A. K.; Harper, J. B. Towards Solvent-Controlled Reactivity in Ionic Liquids. *Pure Appl. Chem.* **2013**, *85*, 1979–1990.
- (6) Weingaertner, H. Understanding Ionic Liquids at the Molecular Level: Facts, Problems, and Controversies. *Angew. Chem., Int. Ed.* **2008**, *47*, 654–670.
- (7) Holloczki, O.; Malberg, F.; Welton, T.; Kirchner, B. On the Origin of Ionicity in Ionic Liquids. Ion Pairing Versus Charge Transfer. *Phys. Chem. Chem. Phys.* **2014**, *16*, 16880–16890.
- (8) Chiappe, C.; Malvaldi, M.; Pomelli, C. S. Ionic Liquids: Solvation Ability and Polarity. *Pure Appl. Chem.* **2009**, *81*, 767–776.
- (9) Castner, E. W.; Wishart, J. F.; Shirota, H. Intermolecular Dynamics, Interactions, and Solvation in Ionic Liquids. *Acc. Chem. Res.* **2007**, *40*, 1217–1227.
- (10) Anderson, J. L.; Ding, J.; Welton, T.; Armstrong, D. W. Characterizing Ionic Liquids on the Basis of Multiple Solvation Interactions. *J. Am. Chem. Soc.* **2002**, *124*, 14247–14254.
- (11) Părvulescu, V. I.; Hardacre, C. Catalysis in Ionic Liquids. *Chem. Rev.* **2007**, *107*, 2615–2665.
- (12) Haumann, M.; Riisager, A. Hydroformylation in Room Temperature Ionic Liquids (RTILs): Catalyst and Process Developments. *Chem. Rev.* **2008**, *108*, 1474–1497.
- (13) Zahn, S.; Brehm, M.; Brüssel, M.; Hollóczki, O.; Kohagen, M.; Lehmann, S.; Malberg, F.; Pensado, A. S.; Schöppke, M.; Weber, H.; Kirchner, B. Understanding Ionic Liquids from Theoretical Methods. *J. Mol. Liq.* **2014**, *192*, 71–76.
- (14) Lynden-Bell, R. M.; Pópolo, M. G. D.; Youngs, T. G. A.; Kohanoff, J.; Hanke, C. G.; Harper, J. B.; Pinilla, C. C. Simulations of Ionic Liquids, Solutions, and Surfaces. *Acc. Chem. Res.* **2007**, *40*, 1138–1145.
- (15) Skarmoutsos, I.; Welton, T.; Hunt, P. A. The Importance of Timescale for Hydrogen Bonding in Imidazolium Chloride Ionic Liquids. *Phys. Chem. Chem. Phys.* **2014**, *16*, 3675–3685.
- (16) Gabl, S.; Schroder, C.; Steinhauser, O. Computational Studies of Ionic Liquids: Size Does Matter and Time Too. *J. Chem. Phys.* **2012**, *137*, 094501.
- (17) Izgorodina, E. I.; Golze, D.; Maganti, R.; Armel, V.; Taige, M.; Schubert, T. J.; MacFarlane, D. R. Importance of Dispersion Forces for Prediction of Thermodynamic and Transport Properties of Some Common Ionic Liquids. *Phys. Chem. Chem. Phys.* **2014**, *16*, 7209–7221.
- (18) Maginn, E. J. Molecular Simulation of Ionic Liquids: Current Status and Future Opportunities. *J. Phys.: Condens. Matter* **2009**, *21*, 373101.
- (19) Chiappe, C.; Pomelli, C. S. Computational Studies on Organic Reactivity in Ionic Liquids. *Phys. Chem. Chem. Phys.* **2013**, *15*, 412–423.
- (20) Acevedo, O.; Jorgensen, W. L. Quantum and Molecular Mechanical (QM/MM) Monte Carlo Techniques for Modeling Condensed-Phase Reactions. *Wiley Interdiscip. Rev.: Comput. Mol. Sci.* **2014**, *4*, 422–435.
- (21) Acevedo, O.; Jorgensen, W. L. Advances in Quantum and Molecular Mechanical (QM/MM) Simulations for Organic and Enzymatic Reactions. *Acc. Chem. Res.* **2010**, *43*, 142–151.
- (22) Acevedo, O.; Jorgensen, W. L. Solvent Effects on Organic Reactions from QM/MM Simulations. In *Annual Reports in Computational Chemistry*; Spellmeyer, D., Ed.; Elsevier: Amsterdam, 2006; Vol. 2, pp 263–278.
- (23) Allen, C.; McCann, B. W.; Acevedo, O. Ionic Liquid Effects on Nucleophilic Aromatic Substitution Reactions from QM/MM Simulations. *J. Phys. Chem. B* **2014**, DOI: 10.1021/jp504967r.
- (24) Allen, C.; Sambasivarao, S. V.; Acevedo, O. An Ionic Liquid Dependent Mechanism for Base Catalyzed B-Elimination Reactions from QM/MM Simulations. *J. Am. Chem. Soc.* **2013**, *135*, 1065–1072.
- (25) Sambasivarao, S. V.; Acevedo, O. Development of OPLS-AA Force Field Parameters for 68 Unique Ionic Liquids. *J. Chem. Theory Comput.* **2009**, *5*, 1038–1050.
- (26) Acevedo, O.; Jorgensen, W. L.; Evanseck, J. D. Elucidation of Rate Variations for a Diels-Alder Reaction in Ionic Liquids from QM/MM Simulations. *J. Chem. Theory Comput.* **2007**, *3*, 132–138.
- (27) Acevedo, O. Determination of Local Effects for Chloroaluminate Ionic Liquids on Diels-Alder Reactions. *J. Mol. Graphics Modell.* **2009**, *28*, 95–101.
- (28) Senn, H. M.; Thiel, W. QM/MM Methods for Biomolecular Systems. *Angew. Chem., Int. Ed.* **2009**, *48*, 1198–1229.
- (29) van der Kamp, M. W.; Mulholland, A. J. Combined Quantum Mechanics/Molecular Mechanics (QM/MM) Methods in Computational Enzymology. *Biochemistry* **2013**, *52*, 2708–2728.
- (30) Jorgensen, W. L. Foundations of Biomolecular Modeling. *Cell* **2013**, *155*, 1199–1202.

- (31) Klähn, M.; Braun-Sand, S.; Rosta, E.; Warshel, A. On Possible Pitfalls in Ab Initio Quantum Mechanics/Molecular Mechanics Minimization Approaches for Studies of Enzymatic Reactions. *J. Phys. Chem. B* **2005**, *109*, 15645–15650.
- (32) Repasky, M. P.; Chandrasekhar, J.; Jorgensen, W. L. PDDG/PM3 and PDDG/MNDO: Improved Semiempirical Methods. *J. Comput. Chem.* **2002**, *23*, 1601–1622.
- (33) Dewar, M. J. S.; Zoebisch, E. G.; Healy, E. F.; Stewart, J. J. P. AM1: A New General Purpose Quantum Mechanical Molecular Model. *J. Am. Chem. Soc.* **1985**, *107*, 3902–3907.
- (34) Rocha, G. B.; Freire, R. O.; Simas, A. M.; Stewart, J. J. P. RM1: A Reparameterization of AM1 for H, C, N, O, P, S, F, Cl, Br, and I. *J. Comput. Chem.* **2006**, *27*, 1101–1111.
- (35) Vreven, T.; Morokuma, K. Hybrid Methods: Oniom(QM:MM) and QM/MM. *Annu. Rep. Comput. Chem.* **2006**, *2*, 35–51.
- (36) Yockel, S.; Schatz, G. C. Dynamic QM/MM: A Hybrid Approach to Simulating Gas-Liquid Interactions. *Top. Curr. Chem.* **2012**, *307*, 43–67.
- (37) Jorgensen, W. L.; Tirado-Rives, J. Potential Energy Functions for Atomic-Level Simulations of Water and Organic and Biomolecular Systems. *Proc. Natl. Acad. Sci. U. S. A.* **2005**, *102*, 6665–6670.
- (38) Tubert-Brohman, I.; Acevedo, O.; Jorgensen, W. L. Elucidation of Hydrolysis Mechanisms for Fatty Acid Amide Hydrolase and Its Lys142ala Variant Via QM/MM Simulations. *J. Am. Chem. Soc.* **2006**, *128*, 16904–16913.
- (39) Armacost, K.; Acevedo, O. Exploring the Aldol Reaction Using Catalytic Antibodies and “on Water” Organocatalysts from QM/MM Calculations. *J. Am. Chem. Soc.* **2014**, *136*, 147–156.
- (40) Thompson, J. D.; Cramer, C. J.; Truhlar, D. G. Parameterization of Charge Model 3 for AM1, PM3, BLYP, and B3LYP. *J. Comput. Chem.* **2003**, *24*, 1291–1304.
- (41) Vilseck, J. Z.; Sambasivarao, S. V.; Acevedo, O. Optimal Scaling Factors for CM1 and CM3 Atomic Charges in Aqueous RM1-Based Simulations. *J. Comput. Chem.* **2011**, *32*, 2836–2842.
- (42) Dommert, F.; Wendler, K.; Berger, R.; Delle Site, L.; Holm, C. Force Fields for Studying the Structure and Dynamics of Ionic Liquids: A Critical Review of Recent Developments. *ChemPhysChem* **2012**, *13*, 1625–1637.
- (43) Jorgensen, W. L.; Maxwell, D. S.; Tirado-Rives, J. Development and Testing of the OPLS All-Atom Force Field on Conformational Energetics and Properties of Organic Liquids. *J. Am. Chem. Soc.* **1996**, *118*, 11225–11236.
- (44) Kaminski, G. A.; Friesner, R. A.; Tirado-Rives, J.; Jorgensen, W. L. Evaluation and Reparametrization of the OPLS-AA Force Field for Proteins Via Comparison with Accurate Quantum Chemical Calculations on Peptides. *J. Phys. Chem. B* **2001**, *105*, 6474–6487.
- (45) Watkins, E. K.; Jorgensen, W. L. Perfluoroalkanes: Conformational Analysis and Liquid-State Properties from Ab Initio and Monte Carlo Calculations. *J. Phys. Chem. A* **2001**, *105*, 4118–4125.
- (46) Lin, Y.-L.; Aleksandrov, A.; Simonson, T.; Roux, B. An Overview of Electrostatic Free Energy Computations for Solutions and Proteins. *J. Chem. Theory Comput.* **2014**, *10*, 2690–2709.
- (47) Toukmaji, A. Y.; Board, J. A., Jr. Ewald Summation Techniques in Perspective: A Survey. *Comput. Phys. Commun.* **1996**, *95*, 73–92.
- (48) Darden, T.; York, D.; Pedersen, L. Particle Mesh Ewald: An N Log(N) Method for Ewald Sums in Large Systems. *J. Chem. Phys.* **1993**, *98*, 10089–10092.
- (49) Brooks, C. L., III; Pettitt, B. M.; Karplus, M. Structural and Energetic Effects of Truncating Long Ranged Interactions in Ionic and Polar Fluids. *J. Chem. Phys.* **1985**, *83*, 5897–5908.
- (50) Levitt, M.; Hirshberg, M.; Sharon, R.; Daggett, V. Potential Energy Function and Parameters for Simulations of the Molecular Dynamics of Proteins and Nucleic Acids in Solution. *Comput. Phys. Commun.* **1995**, *91*, 215–231.
- (51) McCann, B. W.; Acevedo, O. Pairwise Alternatives to Ewald Summation for Calculating Long-Range Electrostatics in Ionic Liquids. *J. Chem. Theory Comput.* **2013**, *9*, 944–950.
- (52) Hansen, N.; van Gunsteren, W. F. Practical Aspects of Free-Energy Calculations: A Review. *J. Chem. Theory Comput.* **2014**, *10*, 2632–2647.
- (53) Chipot, C.; Pohorille, A. *Free Energy Calculations: Theory and Applications in Chemistry and Biology*; Springer: Berlin, 2007; Vol. 86.
- (54) Zwanzig, R. W. High-Temperature Equation of State by a Perturbation Method. I. Nonpolar Gases. *J. Chem. Phys.* **1954**, *22*, 1420–1426.
- (55) Acevedo, O.; Ambrose, Z.; Flaherty, P. T.; Aamer, H.; Jain, P.; Sambasivarao, S. V. Identification of HIV Inhibitors Guided by Free Energy Perturbation Calculations. *Curr. Pharm. Des.* **2012**, *18*, 1199–1216.
- (56) Sambasivarao, S. V.; Acevedo, O. Computational Insight into Small Molecule Inhibition of Cyclophilins. *J. Chem. Inf. Model.* **2011**, *51*, 475–482.
- (57) Jorgensen, W. L.; Ravimohan, C. Monte Carlo Simulation of Differences in Free Energies of Hydration. *J. Chem. Phys.* **1985**, *83*, 3050–3054.
- (58) Sheppard, A. N.; Acevedo, O. Multidimensional Exploration of Valley-Ridge Inflection Points on Potential Energy Surfaces. *J. Am. Chem. Soc.* **2009**, *131*, 2530–2540.
- (59) Vilseck, J. Z. A. O. Computing Free-Energy Profiles Using Multidimensional Potentials of Mean Force and Polynomial Quadrature Methods. *Ann. Rep. Comput. Chem.* **2010**, *6*, 37–49.
- (60) Acevedo, O. Role of Water in the Multifaceted Catalytic Antibody 4B2 for Allylic Isomerization and Kemp Elimination Reactions. *J. Phys. Chem. B* **2009**, *113*, 15372–15381.
- (61) Jorgensen, W. L.; Chandrasekhar, J.; Madura, J. D.; Impey, W.; Klein, M. L. Comparison of Simple Potential Functions for Simulating Liquid Water. *J. Chem. Phys.* **1983**, *79*, 926–935.
- (62) Hu, Y.; Houk, K. N.; Kikuchi, K.; Hotta, K.; Hilvert, D. Nonspecific Medium Effects Versus Specific Group Positioning in the Antibody and Albumin Catalysis of the Base-Promoted Ring-Opening Reactions of Benzisoxazoles. *J. Am. Chem. Soc.* **2004**, *126*, 8197–8205.
- (63) D’Anna, F.; La Marca, S.; Noto, R. Kemp Elimination: A Probe Reaction to Study Ionic Liquids Properties. *J. Org. Chem.* **2008**, *73*, 3397–3403.
- (64) Na, J.; Houk, K. N.; Hilvert, D. Transition State of the Base-Promoted Ring-Opening of Isoxazoles. Theoretical Prediction of Catalytic Functionalities and Design of Haptens for Antibody Production. *J. Am. Chem. Soc.* **1996**, *118*, 6462–6471.
- (65) Kolthoff, I. M.; Chantooni, M. K., Jr.; Bhowmik, S. Dissociation Constants of Uncharged and Monovalent Cation Acids in Dimethyl Sulfoxide. *J. Am. Chem. Soc.* **1968**, *90*, 23–28.
- (66) Crowhurst, L.; Lancaster, N. L.; Arlandis, J. M. P.; Welton, T. Manipulating Solute Nucleophilicity with Room Temperature Ionic Liquids. *J. Am. Chem. Soc.* **2004**, *126*, 11549–11555.
- (67) Pearson, R. G. Ionization Potentials and Electron Affinities in Aqueous Solution. *J. Am. Chem. Soc.* **1986**, *108*, 6109–6114.
- (68) Hussey, C. L. Room-Temperature Haloaluminate Ionic Liquids - Novel Solvents for Transition-Metal Solution Chemistry. *Pure Appl. Chem.* **1988**, *60*, 1763–1772.
- (69) Lee, C. Diels-Alder Reactions in Chloroaluminate Ionic Liquids: Acceleration and Selectivity Enhancement. *Tetrahedron Lett.* **1999**, *40*, 2461–2464.
- (70) Acevedo, O.; Jorgensen, W. L. Understanding Rate Accelerations for Diels-Alder Reactions in Solution Using Enhanced QM/MM Methodology. *J. Chem. Theory Comput.* **2007**, *3*, 1412–1419.
- (71) Acevedo, O.; Evanseck, J. D. Transition Structure Models of Organic Reactions in Chloroaluminate Ionic Liquids - Cyclopentadiene and Methyl Acrylate Diels-Alder Reaction in Acidic and Basic Melts of 1-Ethyl-3-Methylimidazolium Chloride with Aluminum-(III) Chloride. *ACS Symp. Ser.* **2003**, *856*, 174–190.
- (72) Aggarwal, A.; Lancaster, N. L.; Sethi, A. R.; Welton, T. The Role of Hydrogen Bonding in Controlling the Selectivity of Diels-Alder Reactions in Room-Temperature Ionic Liquids. *Green Chem.* **2002**, *4*, 517–520.
- (73) Chiappe, C.; Pieraccini, D.; Saullo, P. Nucleophilic Displacement Reactions in Ionic Liquids: Substrate and Solvent Effect in the

- Reaction of NaN_3 and KCN with Alkyl Halides and Tosylates. *J. Org. Chem.* **2003**, *68*, 6710–6715.
- (74) D'Anna, F.; Frenna, V.; Pace, V.; Noto, R. Effect of Ionic Liquid Organizing Ability and Amine Structure on the Rate and Mechanism of Base Induced Elimination of 1,1,1-Tribromo-2,2-Bis(Phenyl-Substituted)Ethane. *Tetrahedron* **2006**, *62*, 1690–1698.
- (75) Fontana, G.; Frenna, V.; Lamartina, L.; Natoli, M. C.; Noto, R. Kinetic Study of Methoxide-Promoted Elimination Reactions of Some 1,1,1-Trichloro-2,2-Bis(Phenyl-Substituted)Ethanes. *J. Phys. Org. Chem.* **2002**, *15*, 108–114.
- (76) Saunders, W. H., Jr. Distinguishing between Concerted and Nonconcerted Eliminations. *Acc. Chem. Res.* **1976**, *9*, 19–25.
- (77) Gandler, J. R.; Jencks, W. P. General Base Catalysis, Structure-Reactivity Interactions, and Merging of Mechanisms for Elimination Reactions of (2-Arylethyl)Quinuclidinium Ions. *J. Am. Chem. Soc.* **1982**, *104*, 1937–1951.
- (78) Alunni, S.; Angelis, F. D.; Ottavi, L.; Papavasileiou, M.; Tarantelli, F. Evidence of a Borderline Region between E1cb and E2 Elimination Reaction Mechanisms: A Combined Experimental and Theoretical Study of Systems Activated by the Pyridine Ring. *J. Am. Chem. Soc.* **2005**, *127*, 15151–15160.
- (79) Jones, S. G.; Yau, H. M.; Davies, E.; Hook, J. M.; Youngs, T. G.; Harper, J. B.; Croft, A. K. Ionic Liquids through the Looking Glass: Theory Mirrors Experiment and Provides Further Insight into Aromatic Substitution Processes. *Phys. Chem. Chem. Phys.* **2010**, *12*, 1873–1878.
- (80) Acevedo, O.; Jorgensen, W. L. Solvent Effects and Mechanism for a Nucleophilic Aromatic Substitution from QM/MM Simulations. *Org. Lett.* **2004**, *6*, 2881–2884.
- (81) D'Anna, F.; Frenna, V.; Noto, R.; Pace, V.; Spinelli, D. Study of Aromatic Nucleophilic Substitution with Amines on Nitrothiophenes in Room-Temperature Ionic Liquids: Are the Different Effects on the Behavior of Para-Like and Ortho-Like Isomers on Going from Conventional Solvents to Room-Temperature Ionic Liquids Related to Solvation Effects? *J. Org. Chem.* **2006**, *71*, 5144–5150.
- (82) D'Anna, F.; Marullo, S.; Noto, R. Ionic Liquids/[Bmim][N3] Mixtures: Promising Media for the Synthesis of Aryl Azides by Snar. *J. Org. Chem.* **2008**, *73*, 6224–6228.
- (83) Yau, H. M.; Croft, A. K.; Harper, J. B. Investigating the Origin of Entropy-Derived Rate Accelerations in Ionic Liquids. *Faraday Discuss.* **2012**, *154*, 365–371.
- (84) Yau, H. M.; Barnes, S. A.; Hook, J. M.; Youngs, T. G.; Croft, A. K.; Harper, J. B. The Importance of Solvent Reorganisation in the Effect of an Ionic Liquid on a Unimolecular Substitution Process. *Chem. Commun.* **2008**, 3576–3578.
- (85) Kamerlin, S. C.; Haranczyk, M.; Warshel, A. Progress in Ab Initio QM/MM Free-Energy Simulations of Electrostatic Energies in Proteins: Accelerated QM/MM Studies of pKa, Redox Reactions and Solvation Free Energies. *J. Phys. Chem. B* **2009**, *113*, 1253–1272.
- (86) Hu, H.; Yang, W. Development and Application of Ab Initio QM/MM Methods for Mechanistic Simulation of Reactions in Solution and in Enzymes. *THEOCHEM* **2009**, *898*, 17–30.
- (87) Friesner, R. A.; Guallar, V. Ab Initio Quantum Chemical and Mixed Quantum Mechanics/Molecular Mechanics (QM/MM) Methods for Studying Enzymatic Catalysis. *Annu. Rev. Phys. Chem.* **2005**, *56*, 389–427.
- (88) Jorgensen, W. L.; Tirado-Rives, J. Molecular Modeling of Organic and Biomolecular Systems Using Boss and McPro. *J. Comput. Chem.* **2005**, *26*, 1689–1700.
- (89) Vilseck, J. Z.; Tirado-Rives, J.; Jorgensen, W. L. Evaluation of CMS Charges for Condensed-Phase Modeling. *J. Chem. Theory Comput.* **2014**, *10*, 2802–2812.
- (90) Torras, J.; Seabra Gde, M.; Deumens, E.; Trickey, S. B.; Roitberg, A. E. A Versatile Amber-Gaussian QM/MM Interface through Pupil. *J. Comput. Chem.* **2008**, *29*, 1564–1573.
- (91) Harvey, M. J.; De Fabritiis, G. A Survey of Computational Molecular Science Using Graphics Processing Units. *Wiley Interdiscip. Rev.: Comput. Mol. Sci.* **2012**, *2*, 734–742.
- (92) Acevedo, O.; Jorgensen, W. L. Exploring Solvent Effects Upon the Menshutkin Reaction Using a Polarizable Force Field. *J. Phys. Chem. B* **2010**, *114*, 8425–8430.
- (93) Jiang, W.; Wang, Y. T.; Yan, T. Y.; Voth, G. A. A Multiscale Coarse-Graining Study of the Liquid/Vacuum Interface of Room-Temperature Ionic Liquids with Alkyl Substituents of Different Lengths. *J. Phys. Chem. C* **2008**, *112*, 1132–1139.
- (94) Borodin, O. Polarizable Force Field Development and Molecular Dynamics Simulations of Ionic Liquids. *J. Phys. Chem. B* **2009**, *113*, 11463–11478.
- (95) Schroder, C.; Steinhauser, O. Simulating Polarizable Molecular Ionic Liquids with Drude Oscillators. *J. Chem. Phys.* **2010**, *133*, 154511.
- (96) Yan, T.; Burnham, C. J.; Del-Pópolo, M. G.; Voth, G. A. Molecular Dynamics Simulation of Ionic Liquids: The Effect of Electronic Polarizability. *J. Phys. Chem. B* **2004**, *108*, 11877–11881.
- (97) Yan, T.; Wang, Y.; Knox, C. On the Dynamics of Ionic Liquids: Comparisons between Electronically Polarizable and Nonpolarizable Models II. *J. Phys. Chem. B* **2010**, *114*, 6886–6904.
- (98) Buhl, M.; Chaumont, A.; Schurhammer, R.; Wipff, G. Ab Initio Molecular Dynamics of Liquid 1,3-Dimethylimidazolium Chloride. *J. Phys. Chem. B* **2005**, *109*, 18591–18599.
- (99) Mondal, A.; Balasubramanian, S. Quantitative Prediction of Physical Properties of Imidazolium Based Room Temperature Ionic Liquids through Determination of Condensed Phase Site Charges: A Refined Force Field. *J. Phys. Chem. B* **2014**, *118*, 3409–3422.
- (100) Zhang, Y.; Maginn, E. J. A Simple AIMD Approach to Derive Atomic Charges for Condensed Phase Simulation of Ionic Liquids. *J. Phys. Chem. B* **2012**, *116*, 10036–10048.
- (101) Schroder, C. Comparing Reduced Partial Charge Models with Polarizable Simulations of Ionic Liquids. *Phys. Chem. Chem. Phys.* **2012**, *14*, 3089–3102.
- (102) Tran, C. D.; De Paoli Lacerda, S. H.; Oliveira, D. Absorption of Water by Room-Temperature Ionic Liquids: Effect of Anions on Concentration and State of Water. *Appl. Spectrosc.* **2003**, *57*, 152–157.
- (103) Seddon, K. R.; Stark, A.; Torres, M.-J. Influence of Chloride, Water, and Organic Solvents on the Physical Properties of Ionic Liquids. *Pure Appl. Chem.* **2000**, *72*, 2275–2287.
- (104) Seddon, K. R.; Stark, A. Selective Catalytic Oxidation of Benzyl Alcohol and Alkylbenzenes in Ionic Liquids. *Green Chem.* **2002**, *4*, 119–123.
- (105) Hanke, C. G.; Lynden-Bell, R. M. A Simulation Study of Water-Dialkylimidazolium Ionic Liquid Mixtures. *J. Phys. Chem. B* **2003**, *107*, 10873–10878.
- (106) Jiang, W.; Wang, Y.; Voth, G. A. Molecular Dynamics Simulation of Nanostructural Organization in Ionic Liquid/Water Mixtures. *J. Phys. Chem. B* **2007**, *111*, 4812–4818.
- (107) Brehm, M.; Weber, H.; Pensado, A. S.; Stark, A.; Kirchner, B. Proton Transfer and Polarity Changes in Ionic Liquid-Water Mixtures: A Perspective on Hydrogen Bonds from Ab Initio Molecular Dynamics at the Example of 1-Ethyl-3-Methylimidazolium Acetate-Water Mixtures—Part 1. *Phys. Chem. Chem. Phys.* **2012**, *14*, 5030–5044.
- (108) Brehm, M.; Weber, H.; Pensado, A. S.; Stark, A.; Kirchner, B. Liquid Structure and Cluster Formation in Ionic Liquid/Water Mixtures - an Extensive Ab Initio Molecular Dynamics Study on 1-Ethyl-3-Methylimidazolium Acetate/Water Mixtures - Part 2. *Z. Phys. Chem.* **2013**, *227*, 177–203.
- (109) Acevedo, O.; Jorgensen, W. L. Medium Effects on the Decarboxylation of a Biotin Model in Pure and Mixed Solvents from QM/MM Simulations. *J. Org. Chem.* **2006**, *71*, 4896–4902.
- (110) Bulo, R. E.; Ensing, B.; Sikkema, J.; Visscher, L. Toward a Practical Method for Adaptive QM/MM Simulations. *J. Chem. Theory Comput.* **2009**, *5*, 2212–2221.
- (111) Wendler, K.; Brehm, M.; Malberg, F.; Kirchner, B.; Site, L. D. Short Time Dynamics of Ionic Liquids in AIMD-Based Power Spectra. *J. Chem. Theory Comput.* **2012**, *8*, 1570–1579.
- (112) Brehm, M.; Kirchner, B. Travis - a Free Analyzer and Visualizer for Monte Carlo and Molecular Dynamics Trajectories. *J. Chem. Inf. Model.* **2011**, *51*, 2007–2023.

(113) Holloczki, O.; Firaha, D. S.; Friedrich, J.; Brehm, M.; Cybik, R.; Wild, M.; Stark, A.; Kirchner, B. Carbene Formation in Ionic Liquids: Spontaneous, Induced, or Prohibited? *J. Phys. Chem. B* **2013**, *117*, 5898–5907.